

Near-infrared spectroscopy and imaging: A new approach to assess burn injuries

BY LORENZO LEONARDI, MICHAEL G. SOWA, JERI R. PAYETTE, AND HENRY H. MANTSCH

A RECURRENT PROBLEM in the assessment of thermal injuries is the ability to accurately identify the depth and extent of injury. Generally, the depth of a burn injury determines and is inversely related to the ability of the skin to restore and regenerate itself. Burns involve damage to the dermis in varying amounts, reducing the dermal blood supply and altering the skin hemodynamics. Highly destructive burns have only a marginal residual blood supply to the dermis that may result in ischemia and ultimately necrosis of the dermis. The reepithelialization of the tissue depends on the viable dermis below the burned tissue. Thermal injuries are clinically classified according to the depth of the injury as superficial (epidermal), partial thickness (epidermal and varying levels of dermal), and full thickness (epidermal and dermal). Superficial burns are mild burns whereby the tissue is capable of regenerating the epidermis. Partial-thickness injuries destroy a portion of the dermal layer. However, usually sufficient dermis remains, ensuring that effective reepithelialization occurs with adequate vasculature. Deep-partial and full-thickness injuries involve destruction of the dermal layer, and what little if any remains of the dermis is insufficient to regenerate due to a reduced dermal blood supply. The only alternative in these cases is debridement and surgical intervention. The remaining residual cutaneous blood supply at the dermis following an injury is directly related to the extent or depth of tissue damage. Increased depth of thermal injury means there is a greater portion of damaged vessels, and as a result the transport of blood to the tissue is impaired. Therefore, knowledge of the skin hemodynamics following an injury can define for clinicians the extent and depth of damage.

Current clinical practice involves assessing the burn injury based on the visual appearance of the wound upon admission and reassessing as needed during the early postburn period. Reassessment is necessary by virtue of the dynamic changes occurring in the local microcirculation that do not completely evolve until 48 to 72 hr after injury.¹ In a research environment, biopsies followed by histological examination remain the gold standard for gauging burn depth.² However, the major drawback of this technique is that it provides a static picture of the injury reflecting the extent of tissue damage at the time the biopsy was taken. Since burn injuries are dynamic and change over the early postburn period, a single biopsy taken at the initial assessment of the injury may not accurately predict outcome. For this reason, biopsies are not generally relied upon in the clinical assessment of burn injuries. Several techniques such as thermography,³ laser Doppler,⁴ ultrasound,⁵ and fluorescence⁶ have been developed to assess the magnitude of a burn injury. These techniques aim to distinguish between burns of varying severity. In general, the results from these techniques correlate

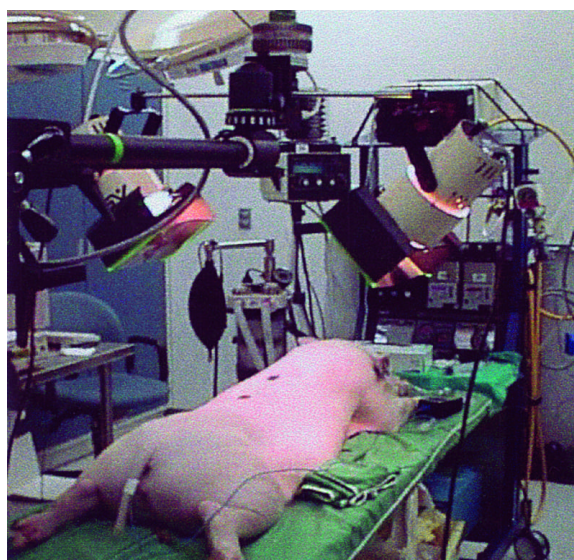


Figure 1 The NIR imaging system provides a rapid and objective assessment of the burn injury.

well with deep or shallow burns; however, the severity of intermediate burns are difficult to assess. Clinically, the key questions lie in the ability to distinguish whether or not the burn injury has the capacity to heal on its own.

A need exists for a reliable, nonsubjective, and easy-to-handle technique to evaluate burn injury hemodynamics in the early postburn period that provides diagnostic as well as prognostic information on the severity of the injury. Near-infrared (NIR) reflectance spectroscopy and imaging provides a noninvasive means of assessing the balance between oxygen delivery and oxygen utilization in tissue. The principal benefit of using NIR spectroscopy and imaging is that regional variations in tissue hemodynamics can be discerned objectively. The main advantage of using NIR light is the extended tissue sampling depth achieved. NIR light (between 700–1100 nm) can penetrate deep within tissue providing vital burn injury-related information. NIR can be used to investigate the epidermis as well as the deep dermis, ideal for burn depth assessment. Thermal injuries disrupt and disturb normal circulation, altering the supply of blood to the tissue. Wound healing involves a number of different processes that must be carried out to accomplish repair. However, many of these processes are dependent on the oxygen delivery to the damaged tissue. Hemoglobin provides an endogenous marker of oxygenation. The oxygenated and deoxygenated states of hemoglobin have different extinction coefficients in the NIR region. Therefore, contained within the NIR absorption spectrum is the relative concentration of both the oxy- and deoxy-hemoglobin. A measure of the combined amounts of oxy- and deoxy-hemoglobin, or total hemoglobin, is related to tissue blood volume, which can be used as an indicator of tissue perfusion while the ratio of oxygenated to total hemoglobin represents the oxygen saturation of tissue.^{7,8,9} The present study uses a porcine model

to demonstrate the potential of NIR spectroscopy and imaging to accurately distinguish between burns of varying severity in the early postburn period based on tissue oxygenation and blood volume changes.

Experimental

NIR imaging

NIR reflectance images of 256×256 pixels were collected between 650 and 1050 nm at 10-nm increments using a Photometrics Series 200 CCD camera (Photometrics, Tucson, AZ) fitted with a Nikon (Melville, NY) Macro AF60 lens and a 7-nm bandpass, full width at half height (FWHM), Lyot-type liquid crystal tunable filter (LCTF) (Cambridge Research Instruments, Cambridge, MA). Each image was acquired with a 200-msec exposure time. The white side of a Kodak Gray Card (Rochester, NY) was used as a reference. Depicted in Figure 1 is the experimental setup with the animal and the spectroscopic imaging system.

NIR depth spectroscopy

NIR spectra were collected with an imaging spectragraph using a multifiber optic bundle (Fiberguide Industries, Stirling, NJ). The multifiber probe consisted of five optical fibers, one to illuminate the tissue and four to collect the reemitted light. The distances of the four collection fibers from the illumination source were 1.5, 3, 4.5, and 6 mm. The illumination optical fiber was coupled with a 100-W quartz tungsten halogen white light source model 77501 (Oriol, Stratford, CT). The four collection optical fibers covering the 500–1100 nm range were placed at the entrance of the imaging spectrograph (Sciencetech Inc., London, Ontario, Canada). A back-thinned, illuminated 1024×128 pixel area image CCD detector model C7041 (Hamamatsu, Bridgewater, NJ), cooled to -10°C , was used as the detection element in the spectrograph. Each image contained the spectrum from all of the four input fibers, which were parsed and binned into four separate raw reflectance spectra. A 99% Spectralon[®] reflectance standard (Lab-Sphere Inc., North Sutton, NH) was used as a reference to convert raw data into reflectance spectra. The measured attenuation is related to the separation distance between the light source and the four detection or collection fibers. The penetration depth of the observed light is dependent on the separation distance between the source and the collector. The further the collector is placed from the source, the greater the depth probed into the tissue.

Animal model

Following a 10-day acclimatization period, adult Yorkshire cross swine weighing between 40 and 50 kg were premedicated with an intramuscu-

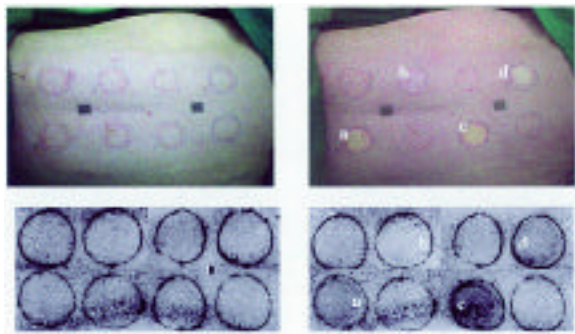


Figure 2 Images describing the preburn (left panels) and postburn (right panels) injuries. The upper panel is a visual (photographic) representation of deep partial-thickness (a), superficial (b), full-thickness (c), and intermediate partial-thickness (d) burns. The lower panels are the corresponding NIR oxygen saturation images.

lar injection of midazolam (0.3 mg/kg), atrophine (0.02 mg/kg), and ketamine (20 mg/kg) as previously reported.¹⁰ Anesthesia was then induced by mask, and the pigs were intubated and mechanically ventilated. Isoflurane (1.5–2.5%) was delivered through the ventilator (via 40–60% oxygen mixed with medical air at 3.0 L/min) to maintain anesthesia for the duration of the experiment. Systemic oxygen saturation, heart rate, and blood pressure were monitored throughout the experiment. Core body temperature was maintained at $39.0\text{ }^{\circ}\text{C} \pm 0.5\text{ }^{\circ}\text{C}$. Blood samples for blood gas and electrolyte analyses were acquired prior to thermal injury and every hour thereafter.

Eight sites, each 3 cm in diameter, were marked on the dorsal surface of the pig as previously described.¹⁰ Burn injuries of varying degrees were then induced on four of the eight sites using a heated brass rod that was 3 cm in diameter. The brass rod was equilibrated in $100\text{ }^{\circ}\text{C}$ water and then applied to the skin with constant pressure (2000 g) for 3, 12, 20, and 75 sec to create superficial, intermediate partial-, deep partial-, and full-thickness burns, respectively. The remaining four uninjured sites were used as controls. The experimental protocol and procedures were approved by the Animal Care Committee at the Institute for Biodiagnostics, National Research Council of Canada (Winnipeg, Manitoba, Canada).

Burn injury assessment

Thermal injuries disrupt the blood flow and oxygen delivery to the damaged tissue. The severe alteration of the microvascular integrity due to a thermal insult results in dramatic hemodynamic changes such as tissue ischemia and impaired tissue perfusion. These factors lead to a relative change and distribution of the levels of oxy- and deoxy-hemoglobin in tissue. These changes can be measured by NIR spectroscopy and used to assess the degree of thermal damage or tissue viability. The relative oxygen saturation (S_tO_2), a measure of the relative amount of oxygenated hemoglobin to the total amount of hemoglobin present (defined as $S_tO_2 = [\text{HbO}_2]/([\text{HbO}_2] + [\text{Hb}])$), provides a quantifiable measure of the oxygen transport in body tissue. The combined measure of oxy- and deoxy-hemoglobin, or total hemoglobin [tHb], is related to tissue blood volume, which can be used as an indicator of tissue perfusion. The oxygenated and deoxygenated forms of hemoglobin have differ-

ent extinction coefficients across the NIR region. Using two or more of the extinction coefficients for oxy- and deoxy-hemoglobin, the S_tO_2 and [tHb] for tissue can be determined from a NIR spectrum of tissue. Hemoglobin concentrations per unit photon pathlength were determined by fitting the absorption coefficients of the oxy- and deoxy-hemoglobin to the observed reflectance attenuation expressed in optical density units over the spectral range of 740–840 nm. The underlying water absorption bands at 730 and 830 nm were subtracted from the spectrum prior to fitting the reflectance attenuation. Oxygen saturation and/or total hemoglobin can be determined from the NIR images and depth-dependent spectroscopic measurements. Each method provides a particular description of the hemodynamic changes occurring within the injured tissue.

Results and discussion

Spectroscopic images

Photographs of the pre- and postburn injuries are reproduced in the upper panels of *Figure 2*. A visual inspection of the wound clearly identifies the superficial burn (*Figure 2*, site b) from the more extensive and severe burns. Assessment of partial and full thickness injuries is difficult and subjective during visual observation in the early postburn period. Tissue oxygen saturation images of the dorsal region of the pig provides a visual survey of tissue oxygenation. The lower panels of *Figure 2* show tissue oxygen saturation images of both the control and burn injuries before and 4 hr after the initial insult. The control sites and surrounding noninvolved tissue appear bright, which indicates normal tissue oxygen saturation. However, the injured sites display a drop in oxygenation following the thermal insult. Sites with low tissue oxygenation appear as dark areas on the dorsum in the postburn S_tO_2 images. However, the site of the superficial injury displays a distinctly different response compared to the more severe burn sites. Oxygenation increases at the superficial burn site in comparison to its preburn levels. This increase corresponds to the visible erythema or tissue reddening associated with minor burns. Hair also appears dark in the oxygen saturation images, but is easily distinguished from areas of tissue with low oxygen saturation.

Depth spectroscopy

Regardless of the degree of injury, all burns show an immediate postinjury alteration in the oxygen saturation and blood volume as displayed in *Figure 3*. The figure summarizes the hemodynamics for the various burn injuries in relation to the source-collector separation or sampling depth into the tissue. All burns exhibit an instantaneous decrease in the tissue oxygenation following the injury. Results from the smallest source-collector separation show no significant difference in the oxygen saturation between burns of different severity relative to the uninjured control tissue. These results were expected since the smaller source-collector separations primarily probe the epidermis. However, the epidermis is mainly avascular depending on the capillary beds in the dermis for oxygen. Thus, there is little or no

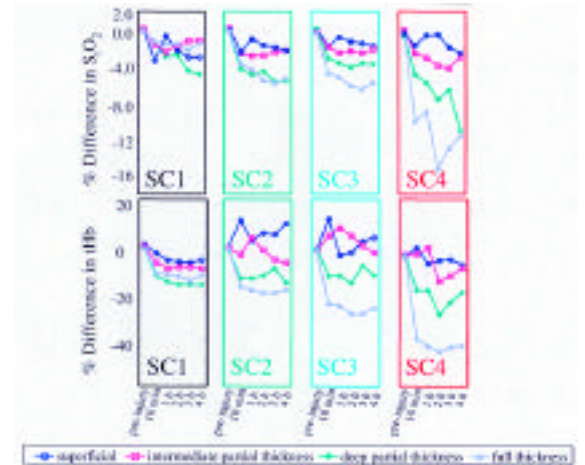


Figure 3 Burn hemodynamics as a function of source-collector (SC) separation during the early postburn period. The top panels denote the oxygen saturation changes and the lower panels the blood volume. The four source-collector separations, denoted SC1 through SC4, correspond to probe separation distances of 1.5, 3, 4.5, and 6 mm.

hemoglobin contribution to the spectral signature from the smallest source-collector separation. As the source-collector separation increases, the tissue sampling depth is extended from the epidermis to the dermis and the burn injuries commence to become discernible. Despite the ability to distinguish oxygenation at various depths, intermediate and deep partial thickness injuries cannot be reliably isolated on the basis of oxygenation measurements.

Total hemoglobin, displayed in the bottom panels of *Figure 3*, provides an efficient indicator of blood volume alterations following a burn injury as a function of probe depth. Again, the burn injuries are indiscernible when probing with the smallest source-collector separation since it is primarily the epidermis that is probed. As the deeper tissue is probed using the larger source-collector separations, the superficial and intermediate partial thickness burns exhibit a notable alteration from the pre-burn state. The immediate 4-hr postburn response from the superficial injuries commences with a sudden increase in blood volume or [tHb], which leads to a hypovolemic state, closely followed by a decrease in blood volume (hypovolemic state) and ending with a steady blood volume increase. Partial thickness injuries also undergo an increase in [tHb]. However, this increase in [tHb] peaks later (2 hr following the injury) and is longer lived than the superficial response. The blood volume changes in the deep partial- and full- thickness injuries are remarkably different from that observed in the less severe injuries. The deep partial wound also demonstrates a hypovolemic peak; however, hypervolemia occurs toward the end of the study. Small source-collector separation distances probe the topmost layer of the skin. This layer has sustained heavy damage with only a limited microcirculation to supply blood to the injured site. By examining deep wounds at these small source-collector separations, one is primarily sampling heavily wounded tissue. On the other hand, large source-collector separations permit sampling of deep tissue, in particular the viable tissue underneath the destroyed visible tissue. Therefore, large source-collector separations are ideally suited to distinguish deep partial- from full-thickness injuries, whereas small source-collector sep-

arations are better suited for distinguishing between superficial and intermediate wounds. Each of the various hemodynamic parameters provides information on the status of the tissue following a thermal insult. Combining several of these parameters along with the added information of the sampling depth, one can isolate and grade the burn injury.

Conclusion

NIR spectral measurements of tissue provide a noninvasive method to distinguish between thermal injuries of varying severity based on hemodynamic parameters related to tissue perfusion (tHb) and oxygen delivery (S_tO_2). The study discussed herein clearly reveals that burns of differing degree have different hemodynamic responses to the thermal insult in the early postburn period. In particular, the physiological parameters of oxygen saturation and total hemoglobin as determined from a time series of NIR reflectance spectra can be used to differentiate the thermal injuries. Burn injuries were identified based on the relative change and distribution in oxygen content and blood volume 4 hr postinjury. Oxygen saturation images provide spatially related hemodynamic changes occurring with thermal damage.

These images are an effective means of localizing the burn and assessing the total surface area of the damaged tissue. Oxygen saturation images can be used to identify near-surface to subsurface physiological changes. Tissue survival is inherently dependent on the available viable tissue underneath the annihilated tissue. Thermal injuries alter the oxygen content and blood perfusion of the tissue. Assessing the varying levels of viable tissue from the different injuries requires spectroscopic sampling at various depths into the tissue. Depth-dependent spectroscopy has been shown to determine oxygen saturation and blood volume changes deep within thermally injured tissue. Burn injuries were identified based on the relative change and distribution in oxygen content and blood volume at various depths into the tissue. NIR spectroscopy may provide clinical personnel with a useful tool in the assessment and evaluation of burns.

References

1. Jackson DM. The diagnosis of the depth of burning. *Br J Surg* 1953; 40:588-96.
2. Chvapil M, Speer DP, Owen JA, Chvapil TA. Identification of the depth of burn injury by collagen stainability. *Plast Reconstr Surg* 1984; 73:438-41.
3. Mason BR, Graff AJ, Pegg SP. Colour thermography in the diagnosis of the depth of burn injury. *Burns* 1981; 7:197-202.
4. Park D, Hwang J, Jang K, Han D, Ahn K, and Baik B. Use of laser doppler flowmetry for estimation of the depth of burns. *Plast Reconstr Surg* 1998; 101:1516-23.
5. Brink JA, Sheets PW, Dines KA, Etchison MR, Hanke CW, and Sadove AK. Quantitative assessment of burn injury in porcine skin with high-frequency ultrasonic imaging. *Invest Radiol* 1986; 21:645-51.
6. Gatti JE, LaRossa D, Silverman DG, and Hartford CE. Evaluation of the burn wound with perfusion fluorometry. *J Trauma* 1983; 23:202-6.
7. Sowa MS, Mansfield JR, Scarth GB, and Mantsch HH. Noninvasive assessment of regional and temporal variations in tissue oxygenation by near infrared spectroscopy and imaging. *Appl Spectr* 1997; 51:143-52.
8. Stranc MF, Sowa MG, Abdulrauf B, Mantsch HH. Assessment of tissue viability using near-infrared spectroscopy. *Br J Plast Surg* 1998; 51(3):210-7.
9. Thorniley MS, Simpkin S, Barnett NJ, et al. Applications of NIRS for measurements of tissue oxygenation and haemodynamics during surgery. *Adv Exp Med Biol* 1997; 411:481-93.
10. Sowa MG, Leonardi L, Payette JR, Fish JS, and Mantsch HH. Near infrared spectroscopic assessment of hemodynamic changes in the early post-burn period. *Burns*, in press.

The authors are with the Institute for Biodiagnostics, National Research Council of Canada, 435 Ellice Ave., Winnipeg, Manitoba, Canada, R3B 1Y6; tel.: 204-984-5195; fax: 204-984-5472; e-mail: larry.leonardi@mrc.ca. These studies were approved by the Animal Care Committee of the Institute for Biodiagnostics of the National Research Council of Canada as protocol 1998-27.